Crystal Structures of Substrates and Products Bound to the Phosphoglycerate Kinase Active Site Reveal the Catalytic Mechanism†

Bradley E. Bernstein and Wim G. J. Hol*

Departments of Biochemistry and Biological Structure and Howard Hughes Medical Institute, Biomolecular Structure Center, University of Washington, Box 357742, Seattle, Washington 98195

Received September 29, 1997; Revised Manuscript Received December 29, 1997

ABSTRACT: Phosphoglycerate kinase (PGK) catalyzes the reversible phosphoryl transfer between 1,3-bisphosphoglycerate and ADP to form 3-phosphoglycerate and ATP in the presence of magnesium. The detailed positions of the substrates during catalysis have been a long-standing puzzle due to the major conformational changes required for active site formation. Here we report the refined closed form *Trypanosoma brucei* PGK ternary complex at an improved resolution of 2.5 Å, together with the crystal structure of closed form *T. brucei* PGK in complex with the nucleotide analogue AMP-PNP. In the 180 000 Da asymmetric unit of the ternary complex, four closed form PGK molecules appear to be arranged as two asymmetric dimers. Quite surprisingly, each dimer is comprised of one 3-phosphoglycerate·MgADP·PGK ternary complex and one P_i·MgADP·PGK pseudoternary complex. The substrates in the ternary complex are bound in a fashion nearly identical to that in open form PGK, but a 30° hinge bending conformational change has brought them together and in-line for catalysis. The pseudoternary complex subunits exhibit a similar hinge closure but contain, instead of 3-phosphoglycerate, a single phosphate molecule bound in the active site. This phosphate binds to a site expected for the 1-position phosphate of 1,3-bisphosphoglycerate, hence providing information for the binding mode for this chemically unstable substrate. The structure of the binary PGK·MgAMP-PNP complex indicates the binding mode for MgATP. An examination of the interactions made by the transferring phosphate groups of the substrate, 1,3-bisphosphoglycerate, and the product, ATP, reveals that in each case only two of the three nonbridging phosphate oxygens are stabilized by hydrogen bonds. In contrast, a model of the transition state phosphoryl group based on all available structural data reveals active site stabilization of all three negatively charged phosphoryl oxygens. These structural models provide insight into the nature of the phosphoryl-transfer reaction catalyzed by PGK and related enzymes.

The glycolytic enzyme phosphoglycerate kinase (PGK) catalyzes the reversible transfer of a phosphoryl group from 1,3-bisphosphoglycerate (1,3-BPG) to ADP, yielding 3-phosphoglycerate (3-PGA) and ATP. Early crystallographic investigations of PGK (*1*, *2*) revealed that this enzyme contains N- and C-terminal domains connected by a narrow hinge region (Figure 1). The triose sugar binds to a site on the N-terminal domain, as demonstrated by the porcine 3-PGA·PGK binary complex (*3*), while the nucleotide binds to the C-terminal domain as documented by the *Bacillus stearothermophilus* ADP·PGK complex (*4*). Bound in this way, the substrates reside more than 10 Å apart, a distance that is incompatible with catalysis. However, an extensive conformational change occurs prior to catalysis that brings the PGK domains and their bound substrates together and in-line for phosphoryl transfer as proved by recent studies of the enzyme from the sleeping sickness parasite *Trypanosoma brucei* (*5*) and confirmed by studies of the enzyme

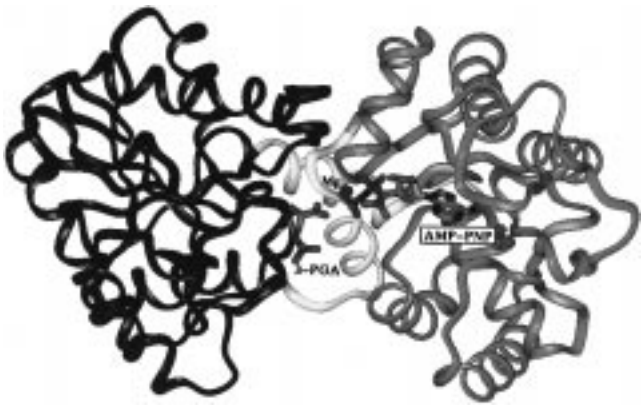

FIGURE 1: Closed form *T. brucei* PGK depicted as a ribbon diagram. The N-terminal domain (residues 5−194 and 411−419) is shown in blue, the C-terminal domain (residues 211−394) in red, and the hinge region (residues 195−210 and 395−410) in yellow. In the stick figure are the products of the PGK reaction represented by 3-PGA, as bound to the ternary complex, and the ATP analogue AMP-PNP, as bound to the AMP-PNP binary complex. The distance between the phosphorus of the transferred γ-phosphate and the O1 carboxylate atom leaving group of the 3-PGA is 3.0 Å, a distance that is indicative for direct phosphoryl transfer.

† We are grateful to the Murdock Charitable Trust and the School of Medicine for equipment funds, to SSRL for synchrotron beam time, and to the Poncin Scholarship Fund which supported B.E.B.

* Author to whom correspondence should be addressed at the Department of Biological Structure and Howard Hughes Medical Institute, Biomolecular Structure Center.

S0006-2960(97)02411-2 CCC: $15.00
Published on Web 03/17/1998

from *Thermotoga maritima* (*6*). In this way, PGK catalysis is selective since active site formation occurs only once both substrates have bound.

Considerable efforts have been directed at understanding the reaction mechanism utilized by PGK and similar enzymes. Isotopic stereochemical experiments demonstrate that the phosphoryl-transfer reaction catalyzed by PGK, and many related enzymes, proceeds by inversion of configuration, thus implicating a direct transfer mechanism with no phosphoenzyme intermediate (*7*, *8*). Direct transfer can proceed via a continuum of transition states ranging from fully dissociative in character to fully associative. A dissociative transition state is characterized by cleavage of the bond between the transferring phosphorus atom and the leaving group prior to formation of the nucleophile bond (*9*). In this scenario, there would be a transient loss of charge on the transferring phosphoryl group and enzyme catalysis would involve the stabilization of negative charge on the leaving group. In contrast, an associative transfer is characterized by bond formation prior to cleavage (*9*). This bond formation would result in increased negative charge on the transferring group, and catalysis would, in this case, rely on the stabilization of negative charge on the phosphoryl group (*10*). Although uncatalyzed phosphoryl transfer proceeds via a dissociative transition state (*9*, *10*), the pathway for enzyme-catalyzed transfer remains to be definitively established in the case of phosphoglycerate kinase.

We are studying *T. brucei* PGK not only as an excellent target for the design of new sleeping sickness drugs (*11*) but also as a model system for understanding at least one potential route by which phosphoryl transfer can proceed. The three-dimensional structure of the closed PGK conformation was revealed by the 2.8 Å *T. brucei* PGK ternary complex (*5*). This abortive ternary complex contains the product 3-PGA and the substrate MgADP bound to the fully formed active site and offers insight into the catalytic elements of the PGK reaction. Here we report new crystallographic data indicating the binding modes also for the substrate 1,3-BPG and the product ATP that has allowed us to investigate the pathway of phosphoryl transfer from a structural and mechanistic perspective and present a detailed view of PGK catalysis.

MATERIALS AND METHODS

Crystallization. *T. brucei* PGK was expressed in *Escherichia coli* and purified to homogeneity as described (*12*). Crystals of the ternary complex were grown at 10 °C by the vapor diffusion method by combining 8 μL of protein solution containing 6 mg/mL PGK plus 10 mM 3-PGA, 10 mM MgADP, 25 mM Tris, pH 7.5, 50 mM NaCl, and 10 mM DTT with an equal volume of well solution containing 2.5 M potassium sodium phosphate at pH 8.0. Crystals of the complex with MgAMP-PNP were grown at room temperature by vapor diffusion by combining 8 μL of protein solution containing 6 mg/mL PGK plus 10 mM MgAMP-PNP, 25 mM Tris, pH 7.5, 50 mM NaCl, and 10 mM DTT with an equal volume of well solution of 2.5 M potassium sodium phosphate at pH 7.5.

Data Collection. Crystals were initially screened on an in-house R-AXIS area detector. All data used in refinement were collected on beamlines 7-1 and 9-1 at the Stanford Synchrotron Radiation Laboratories and processed using DENZO and SCALEPACK (*13*). A single PGK ternary complex crystal was cryopreserved by quickly dipping it into a cryoprotectant solution containing 2.5 M potassium sodium phosphate at pH 8.0 plus 15% erythreitol and flash frozen in a nitrogen gas stream. The crystal belongs to space group $P2_12_12_1$ with unit cell dimensions $a = 111.5$ Å, $b = 113.5$ Å, and $c = 167.9$ Å and a $V_m = 2.9$ Å^3/Da for four molecules in the asymmetric unit. With four 45 kDa subunits and bound substrates, the asymmetric unit contains more than 180 kDa. The R_{merge} is 6.1% for data between 30.0 and 2.5 Å that is 98.5% complete. A single crystal of the MgAMP-PNP·PGK complex was cryopreserved by quickly dipping it into a cryoprotectant solution containing 3.5 M potassium sodium phosphate at pH 7.5. This crystal appears to be nearly isomorphous with the ternary complex crystals and has unit cell dimensions $a = 111.6$ Å, $b = 115.8$ Å, and $c = 167.3$ Å. The R_{merge} is 9.7% for data between 30.0 and 3.15 Å that is 93.8% complete.

Structure Determination and Refinement. The ternary complex crystal structure was solved at 2.5 Å resolution by molecular replacement with AMoRe (*14*) using a single subunit of closed form *T. brucei* PGK refined at 2.8 Å (*5*) as a search probe. Positional, simulated annealing and overall anisotropic *B*-factor and individual restrained *B*-factor refinements were performed using X-PLOR (*15*) and imposed 4-fold noncrystallographic symmetry restraints separately on residues from the N-terminal and C-terminal PGK domains. For model building the program O was used on Silicon Graphics workstations (*16*). In the early stages of refinement, the substrate MgADP was modeled into density for all four subunits. Two 3-PGA and two phosphate molecules were modeled into convincing density at later stages. After refinement was nearly complete, a $(2F_o - F_c)$ electron density map revealed a continuous stretch of unexplained density that extended from the Cβ atom of Ala 98 in all four subunits in the asymmetric unit. The density could be modeled by replacing this alanine residue by an arginine, and a reanalysis of the original sequencing gel of native *T. brucei* glycosomal PGK showed, gratifyingly, that this residue is indeed an arginine.[1] The final model contains 1660 protein residues, 4 molecules of ADP, 4 magnesium ions, 2 molecules of 3-PGA, 2 active site phosphates, 4 additional phosphates located away from the active site, and 599 water molecules. The *R*-factor and *R*-free are currently 22.1% and 29.1%, respectively. A Ramachandran plot analysis by PROCHECK (*17*) indicates that 90.3% of the residues lie in favorable regions and 9.7% in allowed regions.

The MgAMP-PNP·PGK complex was solved at 3.15 Å resolution by rigid body refinement using the protein coordinates for the ternary complex described above. After positional refinement, two MgAMP-PNP molecules were built into good density. After further positional and restrained *B*-factor refinement, the *R*-factor and *R*-free are 22.2% and 28.1%, respectively. A PROCHECK analysis of this structure indicates that 85.1% of residues lie in favorable regions of the Ramachandran plot and 14.9% in allowed regions. Data collection and refinement statistics for both structures are presented in Table 1.

[1] Paul A. M. Michels, personal communication.

Table 1: Crystallographic Data and Refinement Statistics of *T. Brucei* PGK Substrate and Product Complexes

cocrystallized substrates	3-PGA/ MgADP	MgAMP−PNP
space group	$P2_12_12_1$	$P2_12_12_1$
unit cell parameters (Å; *a*, *b*, *c*)	111.5, 113.5, 167.9	111.6, 115.8, 167.3
V_m (Å^3/Da)	2.9	2.9
resolution range (Å)	30.0−2.5	30.0−3.15
unique reflections	73223	37119
data completeness (%)	98.5	93.8
R_{sym} ($\Sigma\|I_{obs} - I_{av}\|/\Sigma\|I\|$) (%)	6.1	9.7
refinement resolution range (Å)	8.0−2.5	8.0−3.15
refined atoms in complex	12652	12638
solvent molecules	599	0
reflections (test set)	64742 (4882)	33265 (2549)
R-factor (*R*-free) (%)	22.1 (29.1)	21.5 (28.9)
mean protein temperature factor (Å^2)	47.6	27.0
mean substrate temperature factor (Å^2)	43.1	26.4
rmsd from ideality in bond lengths (Å)	0.012	0.010
rmsd from ideality in bond angles (deg)	1.6	1.5

RESULTS AND DISCUSSION

The refinement of the *T. brucei* PGK ternary complex using a new data set at higher resolution and with almost 50% more reflections than the original reported structure by Bernstein et al. (*5*) has revealed numerous details not previously elucidated. In particular, the improved data has enabled an investigation of the intersubunit differences among the four PGK molecules in the asymmetric unit of the ternary complex crystals. Although *T. brucei* PGK is a monomer in solution (*18*), these four molecules are arranged as a pair of dimers. Each monomer resides in a slightly different conformation with hinge angles varying by as much as 6°. Conformational differences are restricted to the hinge region of the molecules, while the individual N- and C-terminal domains are highly conserved among the different subunits. This is illustrated by the fact that rms deviations calculated for Cα atoms between entire PGK subunits in the four ternary complexes vary between 0.3 and 0.8 Å, whereas rms deviations calculated between the individual domains range from 0.1 to 0.3 Å.

The most important difference between subunits relates to the type of ligands bound. Although excellent density for MgADP is present in all four cases, convincing density for the 3-PGA substrate only appears in two of the four subunits (Figure 2a). Difference maps of the triose sugar binding sites show that the other two subunits each contain similar spheres of density near the N-termini of helices 13 and 14 in the center of the PGK active site (Figure 2b). The ternary complex crystals were grown from 2.5 M potassium sodium phosphate. A phosphate molecule fits this density well and refines to an average temperature factor of 63.8 Å^2, a reasonable value in comparison with an average *B*-factor of 47.6 Å^2 over all protein atoms. Positioned in this way this phosphate is stabilized by the guanidinium group of Arg 39, by the N-terminus of helix 13, and by the magnesium ion liganded to the bound ADP (see Table 2). The assignment of this density to a phosphate is also supported by the fact that no other potential compounds in the crystallization experiment could fit this sphere. Hence, these subunits form two P_i·MgADP pseudoternary PGK complexes. Interestingly, one "pseudoternary" complex subunit combines with one 3-PGA·MgADP true ternary complex subunit to form the dimer that is observed twice in the asymmetric unit.

The binding site adopted by the inorganic phosphate in the pseudoternary complex subunits appears to provide important information about substrate binding. It resides adjacent to the O3 oxygen of the β-phosphate of the bound ADP (Figure 2b). One inorganic phosphate oxygen atom is directed precisely away from this O3 oxygen, with the other oxygens directed radially in a manner reminiscent of the GDP·phosphate ternary G-protein complex (*19*). In the PGK pseudoternary complex this inorganic phosphate is stabilized by Arg 39 and the backbone amide of Gly 376. In addition, it forms a third ligand for the magnesium ion bound to ADP (Figures 2b and 3a). This magnesium ion has moved 0.8 Å from its position in the ternary complex but remains liganded to the protein via the carboxylate of Asp 377 and also remains close to nonbridging oxygens of the α- and β-phosphates of ADP (Figure 2b). Hence the magnesium seems to play a key role in catalysis.

An analysis of this bound inorganic phosphate in the context of the bound true substrate, 3-PGA, yields an intriguing result. When the C-terminal domains and their bound MgADP substrates from the true ternary complex and the pseudoternary complex are superimposed, the inorganic phosphate assumes a position immediately adjacent to the 3-PGA carboxylate (Figure 3a). Moreover, one of the phosphate oxygens actually sits right on top of the 3-PGA O1 position carboxylate oxygen that is the leaving group for this reaction. Since it is this oxygen that binds to the 1-position phosphate in 1,3-BPG, it appears that the binding mode for this chemically unstable substrate is revealed by combining the structures of the ternary 3-PGA·ADP and the pseudoternary P_i·ADP PGK complexes.

The ternary complex structure documents, therefore, the binding of both PGK substrates (1,3-BPG and ADP) as well as one of its products (3-PGA). The binding mode for the second product, ATP, was determined by cocrystallizing *T. brucei* PGK with the nonhydrolyzable ATP analogue AMP-PNP (Figure 2c). Conveniently, this complex forms crystals under similar conditions with PGK again assuming a closed conformation. It was initially unexpected that cocrystallization with AMP-PNP alone should yield closed form PGK crystals. However, this crystallization was performed in the presence of high concentrations of phosphate which appears to serve, like 3-PGA, to induce closure of this enzyme. This observation is consistent with neutron scattering experiments that indicate that the presence of anions significantly decreases the radius of gyration of PGK (*20*). Furthermore, we have also crystallized a *T. brucei* PGK·inhibitor complex in the presence and absence of phosphate and found, again, that the presence of this anion facilitates hinge closure.[2]

Notwithstanding, the AMP-PNP binary complex reveals the binding mode for the product ATP in the context of the PGK active site. A comparison with bound ADP reveals that adenosine binding is virtually identical in both cases. Despite a slight rearrangement of the α-phosphate, the β-phosphate group of the triphosphate nucleotide analogue assumes a position very similar to that in ADP (Figure 2a,c). As expected, the transferring γ-phosphate attached to the O3

[2] Bernstein et al., manuscript in preparation.

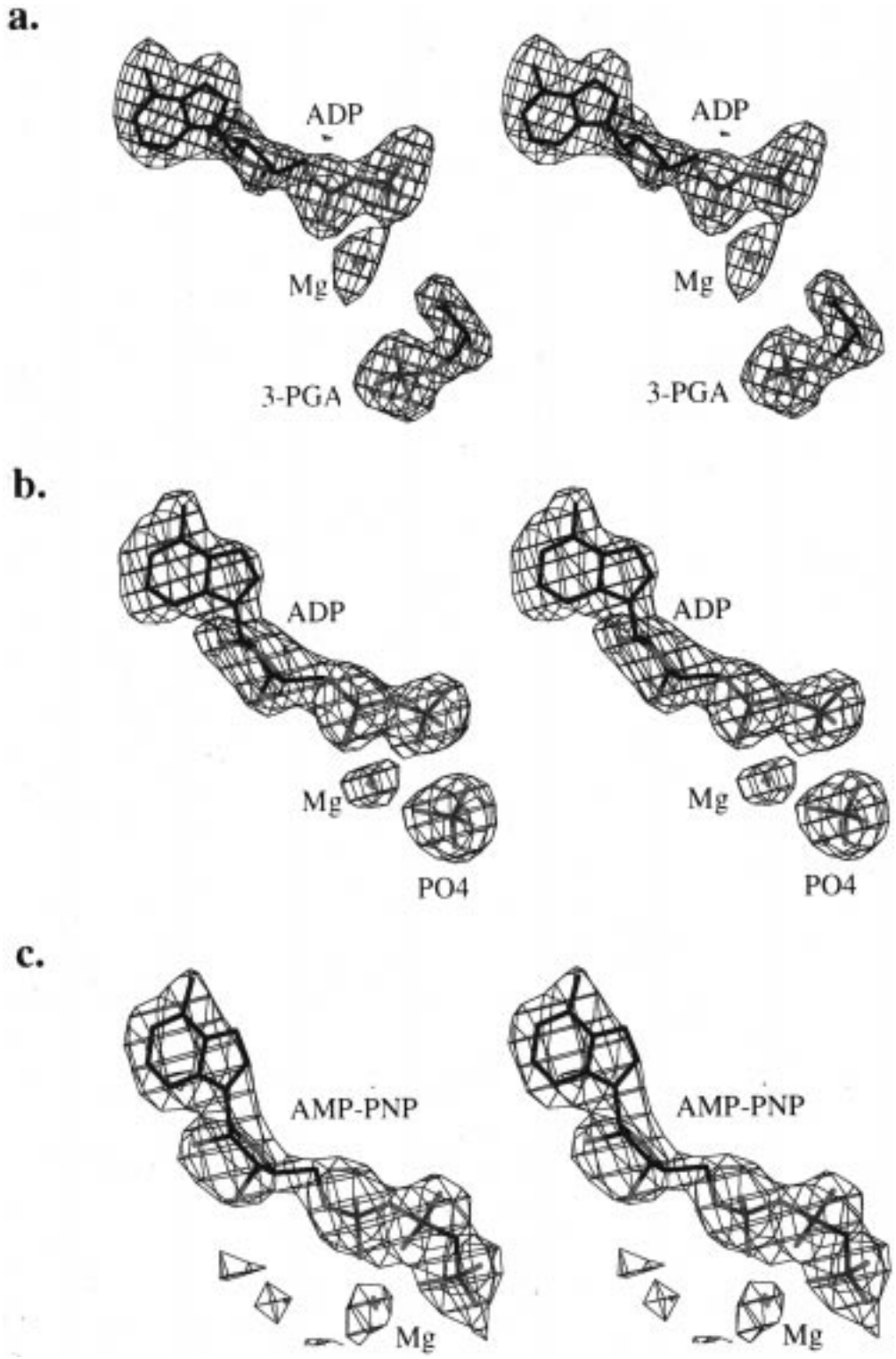

FIGURE 2: Substrates bound in the PGK active site shown in stereoview. Electron density omit maps are contoured at 3σ and shown with substrates for (a) the ternary 3-PGA·MgADP·PGK complex, (b) the pseudoternary P_i·MgADP·PGK complex, and (c) the binary MgAMP-PNP·PGK complex.

oxygen of the β-phosphate is directed precisely toward the position occupied by the O1 nucleophile of 3-PGA in the PGK ternary complex. Also of interest is the position assumed by the magnesium ion bound to the triphosphate nucleotide in the AMP-PNP·PGK complex. It appears that this required divalent cation is liganded to three oxygens, one from each nucleotide phosphate group. In comparison to its position in the context of ADP, the magnesium has moved 1.5 Å. This movement is combined with a 1.2 Å shift of the Asp 377 carboxylate oxygen away from the cation, and, as a consequence, the magnesium is no longer liganded to this protein residue. This finding is consistent with equilibrium dialysis experiments which show that while the affinity of ADP for phosphoglycerate kinase is increased in the presence of magnesium, the affinity of ATP is not affected by this cation (*21*). The observation that, in the context of trinucleotide, the magnesium is not directly liganded to protein has also been confirmed by the 2.0 Å

Table 2: Observed Key Contact Distances for *T. Brucei* PGK in Complex with 3-PGA·ADP, P_i·ADP, and AMP-PNP

		distances (Å)				
ligand atom	protein atom	TC 1[a]	TC 2[a]	PC 1[b]	PC 2[b]	AMP-PNP
nucleotide β-PO1	Ser 378 NH	3.0	2.9	2.8	3.1	
nucleotide β-PO1	Ser 378 Oγ	2.6	2.9	2.8	2.6	3.1
nucleotide β-PO2	Asp 377 NH	3.1	2.8	2.9	2.8	2.9
nucleotide β-PO3	Asn 338 ND2	3.2	3.1	3.1	3.0	
nucleotide γ-PO1	Gly 399 NH					3.2
Mg^{2+}	Asp 377 OD2	2.7	2.3	2.7	2.1	
P_i O2	Arg 39 NH1			2.9	2.8	
P_i O2	Gly 376			2.9	3.1	
3-PGA O2	Asn 26 ND2	2.9	3.1			
3-PGA O2	Arg 39 NH	3.0	3.3			

[a] Ternary complex subunits 1 and 2. [b] Pseudoternary complex subunits 1 and 2.

crystal structure of *T. maritima* PGK with AMP-PNP (*6*).

Armed with crystallographic evidence for the binding modes of all substrates and products to the fully formed PGK active site, we began to investigate the mechanism of phosphoryl transfer in this enzyme. The various PGK subunits in the ternary/pseudoternary complex crystals and in the AMP-PNP binary complex crystals assume different hinge bending conformations that vary in hinge angle by as much as 6°. The most closed subunit turned out to be a true ternary 3-PGA·ADP·PGK complex subunit which differs by only 2° from the second true ternary complex. Both true ternary complexes are highly similar in active site conformation and in their ligand binding. The most closed complex contains the very best active site density and was therefore chosen as a basis for this mechanistic investigation. The interatomic distance between nucleophile and leaving group oxygens (i.e., O3 of ADP and O1 carboxylate of 3-PGA) in this complex is 4.6 Å, an ideal distance for the direct in-line phosphoryl-transfer reaction implicated in PGK.

Using this ternary complex subunit as a foundation, the pseudoternary complex substrates were overlayed onto the 3-PGA·ADP·PGK complex active site by superimposing ADP atoms. As described previously, this treatment places the inorganic phosphate molecule adjacent to the 3-PGA substrate to essentially form 1,3-BPG. Furthermore, the PGK substrates 1,3-BPG and ADP now reside adjacent to one another, with the O3 oxygen of the ADP β-phosphate in a position to act as the nucleophile in the capture of the incoming phosphorus molecule which lies 3.5 Å away. Two of the three oxygens on the 1-position phosphate of 1,3-BPG are stabilized. One oxygen forms hydrogen bonds with the backbone amide of Gly 376 at 2.9 Å and the guanidinium group of Arg 39 at 2.6 Å (Figure 3a). A second oxygen interacts with the positively charged magnesium ion at a distance of 2.8 Å. However, the role of the magnesium ion in the PGK reaction has been disputed (*6*). Our model of PGK in the context of bound substrates provides evidence that the magnesium ion bridges the substrates. This finding is consistent with ^{31}P NMR studies that indicate that the divalent cation becomes coordinated to both nucleotide and triose phosphate substrate (*22*). Bridging the substrate in this way, the cation is in excellent position to assist in catalysis by stabilizing the transferring phosphoryl group.

Next, the AMP-PNP from the PGK binary complex was superimposed on the ADP nucleotide to portray this product in the context of the fully closed active site and its bound product, 3-PGA (Figure 3b). Here, the leaving group (O1 carboxyl of the 3-PGA) resides just 3 Å from the phosphorus of the trinucleotide γ-phosphate. Since PGK-catalyzed phosphoryl transfer is reversible, the leaving group can also be considered the nucleophile for the reverse reaction. Like the 1-position phosphate of the substrate 1,3-BPG, the γ-phosphate of the trinucleotide is stabilized by interactions with *two* of its three negatively charged phosphate oxygens. Again, one oxygen interacts with the magnesium at a distance of 2.6 Å, while a second hydrogen bonds to the backbone amide of Gly 399, 3.2 Å away (Figure 3b).

The above models contain therein the transferring phosphate group bound to both substrate (1,3-BPG as represented by the superposition of 3-PGA and P_i) and product (ATP as represented by AMP-PNP) in the context of the PGK active site. When 1,3-BPG and AMP-PNP are superimposed on the same closed form active site, the phosphorus atoms of the transferring phosphates reside 2.0 Å apart. Furthermore, when superimposed in this way, the transferring phosphate groups assume similar but inverted configurations with corresponding oxygens nearly superposed. This is consistent with the direct transfer mechanism implicated for PGK and provides further evidence that the observed structures are catalytically relevant.

The structures of these substrates and products provide an excellent basis on which to model the PGK transition state phosphoryl group and its interactions with the active site. This transition state consists of a trigonal bipyramidal phosphoryl group that is approximately equidistant between leaving group and nucleophile. It was modeled in the context of the PGK active site (Figure 3c) by placing the phosphorus atom of a planar PO_3 group 2.3 Å from both nucleophile (the O3 atom of the ADP β-phosphate) and leaving group (the O1 carboxylate atom of 1,3-BPG). This PO_3 group was oriented by placing the three oxygens at intermediate positions between the corresponding oxygens of the transferring phosphates from 1,3-BPG and AMP-PNP.

This model for the PGK transition state immediately reveals a potential mechanism for PGK catalysis. Most crucially, in PGK all *three* nonbridging transition state oxygens are stabilized by positively charged ligands (Figure 3c), in contrast to a stabilization of only two nonbridging oxygens of the transferring phosphate in either substrate or product as discussed above. One oxygen of the planar transition state PO_3 group forms a hydrogen bond with the backbone amide of Gly 399 at a distance of 3.1 Å, an interaction that is strengthened by the helix dipole effect since Gly 399 resides at the N-terminus of helix 14. A second phosphoryl oxygen is stabilized by two hydrogen bonds, one with the guanidinium group of Arg 39 at a distance of 2.5 Å and a second with the backbone amide of Gly 376 at a distance of 2.8 Å. This latter interaction is also stabilized by the helix dipole effect as Gly 376 is at the N-terminus of helix 13.

Stabilization of the third phosphoryl oxygen appears from our studies to be provided by two elements. First, our model of the transition state phosphoryl group indicates the third phosphoryl oxygen is stabilized by the magnesium and verifies the critical role played by this required cation in PGK catalysis (Figure 3c). In the context of substrates ("1,3-BPG" model and ADP) the magnesium ion assumes a bridging position that is very similar to the position it assumes in the

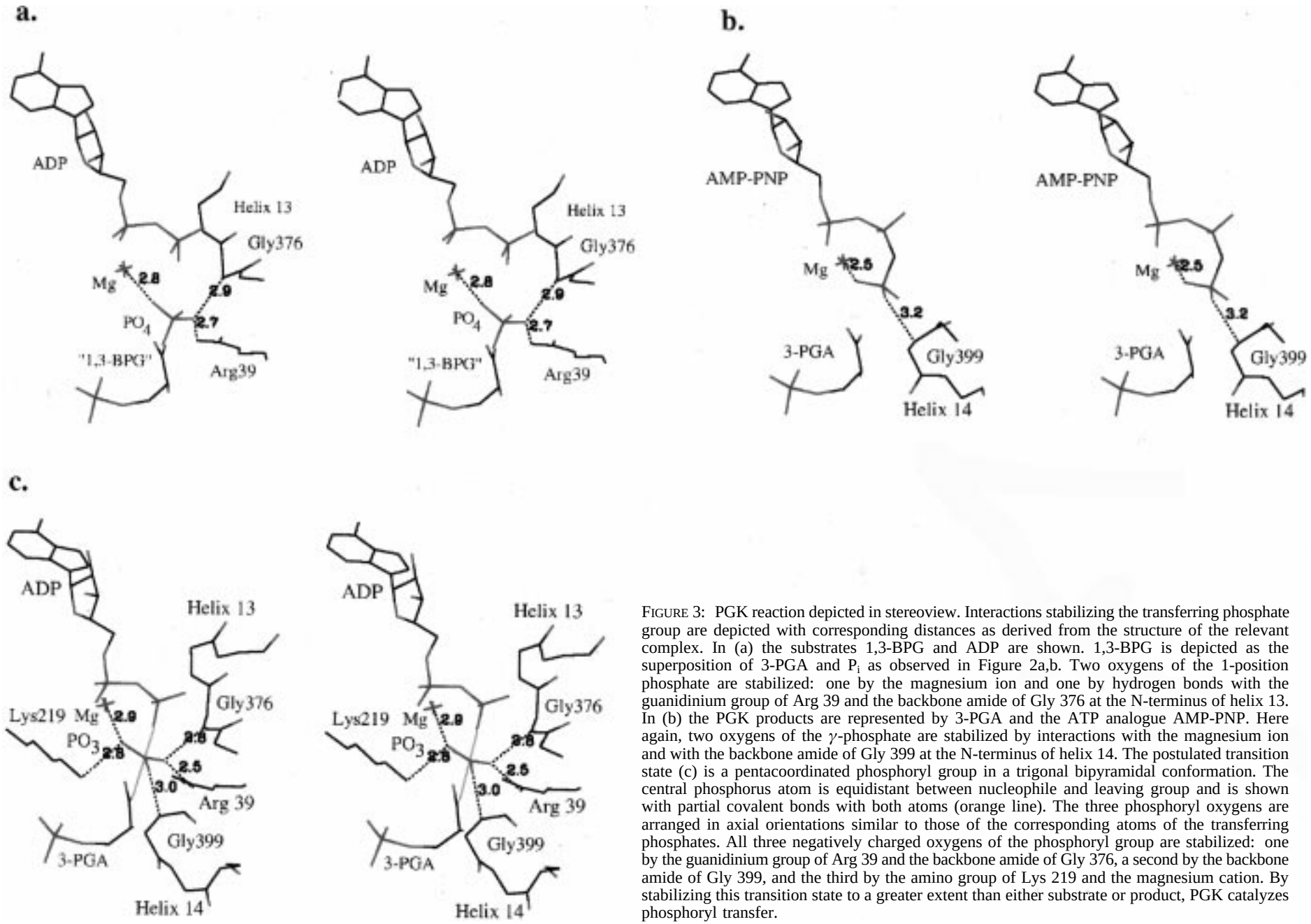

FIGURE 3: PGK reaction depicted in stereoview. Interactions stabilizing the transferring phosphate group are depicted with corresponding distances as derived from the structure of the relevant complex. In (a) the substrates 1,3-BPG and ADP are shown. 1,3-BPG is depicted as the superposition of 3-PGA and P_i as observed in Figure 2a,b. Two oxygens of the 1-position phosphate are stabilized: one by the magnesium ion and one by hydrogen bonds with the guanidinium group of Arg 39 and the backbone amide of Gly 376 at the N-terminus of helix 13. In (b) the PGK products are represented by 3-PGA and the ATP analogue AMP-PNP. Here again, two oxygens of the γ-phosphate are stabilized by interactions with the magnesium ion and with the backbone amide of Gly 399 at the N-terminus of helix 14. The postulated transition state (c) is a pentacoordinated phosphoryl group in a trigonal bipyramidal conformation. The central phosphorus atom is equidistant between nucleophile and leaving group and is shown with partial covalent bonds with both atoms (orange line). The three phosphoryl oxygens are arranged in axial orientations similar to those of the corresponding atoms of the transferring phosphates. All three negatively charged oxygens of the phosphoryl group are stabilized: one by the guanidinium group of Arg 39 and the backbone amide of Gly 376, a second by the backbone amide of Gly 399, and the third by the amino group of Lys 219 and the magnesium cation. By stabilizing this transition state to a greater extent than either substrate or product, PGK catalyzes phosphoryl transfer.

context of the PGK products (3-BPG and AMP-PNP). Furthermore, by assuming this same position, the cation is also in excellent range to stabilize the transition state phosphoryl group. Hence, this cation is able to assist in phosphoryl transfer with minimal change in position during the PGK reaction.

This third transition state phosphoryl oxygen is also stabilized by a second important element. Upon hinge closure, the amino group from Lys 219 comes to reside within hydrogen-bonding distance of a phosphate oxygen of 3-PGA. This is an intriguing interaction in two respects. First, by connecting the C-terminal to the N-terminal domain (to which 3-PGA binds), this interaction may play a role in stabilization of closed form PGK. Second, as pointed out by Auerbach et al., the positively charged amino group is now in range to aid in the stabilization of the phosphoryl-transfer transition state (*6*). Although the side chain of this lysine is not well ordered in the *T. brucei* PGK crystal structures, by placing it in its most favorable conformation we find that the positively charged amino group resides 2.8 Å from the third phosphoryl oxygen (Figure 3c). As shown in Figure 3c, this third transition state oxygen is then very well stabilized by both the magnesium cation and Lys 219.

Hence, the key to PGK catalysis is the following: Upon substrate binding, hinge closure, and active site formation, enzyme ligands stabilize only two of the three oxygens on the transferring phosphate group of the substrate (the 1-position phosphate of 1,3-BPG). On proceeding toward its transition state arrangement, the phosphoryl group finds all three of its oxygens stabilized by enzyme ligands, in addition to being stabilized by the divalent magnesium ion. In this way PGK favors the transition state to a greater extent than either its substrate or its product (the γ-phosphate of ATP), where, again, just two of the phosphate oxygens are stabilized.

On the basis of this structural model for PGK catalysis, the chemical nature of the transition state can now be considered. In the most closed *T. brucei* PGK subunit that has been crystallographically observed, the distance between nucleophile (the O3 atom of the ADP β-phosphate) and leaving group (the O1 carboxylate atom of 1,3-BPG) is 4.6 Å. This finding suggests that the transition state would need to have a decreased bond order in view of the O−P bond distances of ∼2.3 Å. Assuming that no additional hinge closure occurs, the transition state must then be considered to be largely dissociative in character (*9*). On the other hand, like in the GTPase Ras p21 (*23*), the primary effect of the PGK active site appears to be to stabilize negative charge on the transferring phosphoryl group. As proposed by Maegley et al. (*10*), this kind of stabilization of negative charge is consistent with an associative transition state which would require a small further hinge closure of PGK. Hence, it appears that this crystallographic study is unable to definitively differentiate between associative and dissociative phosphoryl transfer and that further chemical and structural studies are warranted.

As a final note, it is worthwhile to consider the similarities between the phosphoryl-transfer reaction catalyzed by PGK and that catalyzed by GTPases and their activating proteins. Specifically, the fully formed PGK active site is similar to that of an activated GTPase in that positively charged residues are in position to stabilize negative charge on the substrates and transition state (*23*, *24*). In both systems, futile hydrolysis of trinucleotides could be a facile and energetically costly side reaction, and it is therefore crucial that both enzymes be highly regulated. In the case of the GTPase Ras p21, regulation is accomplished by the GTPase activating protein, GAP, which introduces a required arginine into the active site (*24*). In PGK, a similarly required arginine, Arg 39, resides on the N-terminal domain and only assumes its final position near the nucleotide once the triose sugar substrate has also bound.

ACKNOWLEDGMENT

We thank P. Michels for providing the PGK overexpression system, S. Sarfaty for help with crystallization, S. Turley for maintaining the in-house data collection facilities, and P. Kuhn, S. Suresh, and M. Redinbo for help with data collection.

REFERENCES

1. Banks, R. D., Blake, C. C. F., Evans, P. R., Haser, R., Rice, D. W., Hardy, G. W., Merrett, M., and Phillips, A. W. (1979) *Nature 279*, 773−777.
2. Watson, H. C., Walker, N. P. C., Shaw, P. J., Bryant, T. N., Wendell, P. L., Fothergill, L. A., Perkins, R. E., Conroy, S. C., Dobson, M. J., Tuite, M. F., Kingsman, A. J., and Kingsman, S. M. (1982) *EMBO J. 1*, 1635−1640.
3. Harlos, K., Vas, M., and Blake, C. F. (1992) *Proteins 12*, 133−144.
4. Davies, G. J., Gamblin, S. J., Littlechild, J. A., Dauter, Z., Wilson, K. S., and Watson, H. C. (1994) *Acta Crystallogr. D50*, 202−209.
5. Bernstein, B. E., Michels, P. A. M., and Hol, W. G. J. (1997) *Nature 385*, 275−279.
6. Auerbach, G., Huber, R., Grattinger, M., Zaiss, K., Schurig, H., Jaenicke, R., and Jacob, U. (1997) *Structure 5*, 1475−1483.
7. Webb, M. R., and Trentham, D. R. (1980) *J. Biol. Chem. 255*, 1775−1779.
8. Knowles, J. R. (1980) *Annu. Rev. Biochem. 49*, 877−919.
9. Cleland, W. W., and Hengge, A. C. (1995) *FASEB J. 9*, 1585−1594.
10. Maegley, K. A., Admiraal, S. J., and Herschlag, D. (1996) *Proc. Natl. Acad. Sci. U.S.A. 93*, 8160−8166.
11. Verlinde, C. L. M. J., Merritt, E. A., van den Akker, F., Kim, H., Feil, I., Delboni, L. F., Mande, S. C., Sarfaty, S., Petra, P. H., and Hol, W. G. J. (1994) *Protein Sci. 3*, 1670−1686.
12. Bernstein, B. E., Michels, P. A. M., Kim, H., Petra, H., and Hol, W. G. J. (1998) *Protein Sci. 7*, 504−507.
13. Otwinowski, Z. (1993) in *Data Collection and Processing* (Sawyer, L., Isaacs, N., and Burley, S., Eds.) pp 56−62, Daresbury Laboratory, U.K.
14. Navaza, J. (1994) *Acta Crystallogr. A50*, 157−163.
15. Brunger, A. T. (1992*) X-PLOR Version 3.1, A system for X-ray crystallography and NMR*, Yale University Press, New Haven, CT.
16. Jones, T. A., Zou, J. Y., Cowan, S. W., and Kjeldgaard, M. (1991) *Acta Crystallogr. A47*, 110−119.
17. CCP4 (1994) *Acta Crystallogr. D50*, 760−763.
18. Misset, O., Bos, O. J. M., and Opperdoes, F. R. (1986) *Eur. J. Biochem. 157*, 441−453.
19. Berghuis, A. M., Lee, E., Raw, A. S., Gilman, A. G., and Sprang, S. R. (1996) *Structure 4*, 1277−1290.

20. Henderson, S. J., Serpersu, E. H., Gerhardt, B. S., and Bunick, G. J. (1994) *Biophys. Chem. 53*, 95−104.
21. Molnar, M., and Vas, M. (1993) *Biochem. J. 293*, 595−599.
22. Pappu, K. M., Gregory, J. D., and Serpersu, E. H. (1994) *Arch. Biochem. Biophys. 311*, 503−508.
23. Scheffzek, K., Ahmadian, M. R., Kabsch, W., Wiesmuller, L., Lautwein, A., Schmitz, F., and Wittinghofer, A. (1997) *Science 277*, 333−338.
24. Rittinger, K., Walker, P. A., Eccleston, J. F., Smerdon, S. J., and Gamblin, S. J. (1997) *Nature 389*, 758−762.

BI9724117